

# Engineering Notes

### Design of Command Limiting Control Law Using Exponential Potential Functions

Donglei Sun\* and Naira Hovakimyan<sup>†</sup>
University of Illinois at Urbana-Champaign, Urbana,
Illinois 61801
and

Hamidreza Jafarnejadsani<sup>‡</sup> Stevens Institute of Technology, Hoboken, New Jersey 07030

https://doi.org/10.2514/1.G004972

#### I. Introduction

A IRCRAFT loss of control is a major cause of aviation accidents and fatalities [1,2]. Flight envelope protection (FEP) is an effective strategy to prevent aircraft loss of control caused by aggressive or excessive pilot/autopilot commands [3,4]. The study of FEP has attracted wide attention in the aerospace control community; see [5–7].

Study on envelope protection is generally focused on two main tasks: violation prediction and violation prevention. To predict possible violations of envelope limit, methods such as neural networks, dynamic trim, and steady-state analysis have been explored [8-13]. Neural networks were used to predict the future value of limited parameters and estimate command or control margins [8–11]. The dynamic trim concept assumes that the fast states of an aircraft such as angular rates are in steady state while the slow states such as attitudes are varying. Based on this concept, the future value of a state can be predicted [12]. In [13], steady-state analysis was conducted to obtain the steady-state values of angle of attack from different reference pitch commands in different flight conditions. These values were then used to compute the maximum reference pitch command. In the latter task, to prevent envelope violations two strategies have been proposed: pilot cueing and direct intervention. In the first strategy, warning signals such as audible, tactile, and visual cues or their combinations are generated to notify the pilot of possible envelope violations, and the pilot has to take effective actions to prevent any violation [8,14,15]. In the second case, the envelope protection module intervenes directly and adjusts the control or command signals to avoid a violation [7,9,13,16]. This paper focuses on the task of direct intervention.

There have been extensive results on direct interventions. In [16], fuzzy logic was employed to develop a control blending logic to mix pilot inputs with limit protection inputs. In [13], a reference command limit was computed and compared with the pilot command input to keep the latter inside the limit. A safe response profile was prescribed close to the boundary in [9], and when an envelope violation was foreseen, corrections to the command/control channel were made following this response profile. Reference [17] proposed a protection method using an inner-loop/outer-loop-type controller that generated constraints on the outer loop command corresponding to the constraints on the inner loop command. Reference [18] presented a switched envelope protection method with several controllers running in parallel with a linear switching logic. The study in [19,20] developed and tested state-limiting systems for the X-48B blended-wing-body aircraft with angle tracking controllers. In this formulation the angle of attack and sideslip angle limiters can modify the damping ratio and natural frequency of the closed-loop systems when the angles are close to their limits, avoiding large overshoot and the associated limit violations. The study in [5] compared several envelope protection approaches for implementation on small aircraft and concluded that for practical implementation, command limiting was superior to control limiting. A command limiting approach was proposed in [21], where the dynamic inversion control laws were used to anticipate limit exceedences, and the scheme switched to a model following control law for envelope protection whenever a limit was about to be violated. An adaptive envelope protection algorithm was presented in [22], where a control architecture involving separate pilot command filtering was employed. A dynamic inversion control architecture coupled with an artificial neural network was proposed in [23] for component damage estimate and control gain adjustment.

In [24], a command limiting strategy based on potential field method was proposed for bank angle protection of an aircraft model with a proportional-integral (PI) roll rate control augmentation system (CAS). The potential field method with a gradient descent algorithm has been widely used in robot motion planning and unmanned aerial vehicle (UAV) path planning to avoid obstacles; see [25-27]. The attractive potential fields drive the vehicle to the goal position while the repulsive potential fields prevent it from colliding with obstacles. Employing a similar idea, in [24] the envelope boundary was treated as a virtual obstacle and a repulsive potential field was constructed close to and beyond it while the pilot reference command played the role of the attractive potential field. A gradient descent rule with the repulsive potential field generated a protection command signal that was superimposed onto the pilot command such that when the protected state was far from the envelope boundary, the pilot command would not be modified, and when the protected state approached the boundary, the pilot command was reduced to prevent a violation of the limit. With this approach, only the measured system states were used by the envelope protection algorithm, and violation prediction was not required. In [28], this method was further improved by including the roll rate into the potential function for enhanced performance.

In both [24,28], a quadratic potential field was used in the design, and the final envelope protection command took the form of either a proportional (P) or a proportional-derivative (PD) attitude tracking control law with a time-varying gain. This result is similar to some methods proposed in other studies [7,29,30]. In these approaches, the reference command was compared with the protection command and the smaller one was sent to the vehicle. In this paper, a command limiting method based on an exponential potential field is explored for systems with an angular rate CAS. With the exponential functions, the FEP command is integrated with the reference command and corrects it directly without any violation prediction. Comparison with the reference command is also not required due to the property of

Presented as Paper 2018-0878 at the AIAA Guidance, Navigation, and Control Conference, Kissimmee, FL, January 8–12, 2018; received 24 November 2019; revision received 25 August 2020; accepted for publication 26 August 2020; published online 9 October 2020. Copyright © 2020 by Donglei Sun, Naira Hovakimyan, and Hamidreza Jafarnejadsani. Published by the American Institute of Aeronautics and Astronautics, Inc., with permission. All requests for copying and permission to reprint should be submitted to CCC at <a href="https://www.copyright.com">www.copyright.com</a>; employ the eISSN 1533-3884 to initiate your request. See also AIAA Rights and Permissions <a href="https://www.aiaa.org/randp">www.aiaa.org/randp</a>.

<sup>\*</sup>Doctoral Student, Department of Aerospace Engineering; dsun13@ illinois.edu. Student Member AIAA.

<sup>&</sup>lt;sup>†</sup>Professor, Department of Mechanical Science and Engineering; nhovakim@illinois.edu. Fellow AIAA.

<sup>\*</sup>Assistant Professor, Department of Mechanical Engineering; hjafarne@stevens.edu.

exponential functions. Stability analysis using Lyapunov theory is provided to justify the design. A simulation example is presented for pitch angle protection of a nonlinear UAV model to verify the design.

The rest of this paper is organized as follows. In Sec. II, the problem of command limiting control law design is formulated. In Sec. III, the command limiting design using exponential potential functions is proposed and analyzed. Simulation examples are discussed in Sec. IV and conclusions are drawn in Sec. V.

#### **II. Problem Formulation**

An *n*th-order linear system in the controllability canonical form is considered, where the first state  $x_1(t)$  needs soft protection such that it should not overshoot excessively over a given limit  $X_m > 0$ . This state can represent the attitude of an aerial vehicle, e.g., the pitch angle. The remaining  $x_i(t)$ ,  $i = 2, 3, \ldots, n-1$  represent other states of the aerial vehicle with a rate CAS. The system is represented by the following equation of motion:

$$\dot{x}(t) = Ax(t) + bx_{2c}(t), \qquad x(0) = x_0$$
 (1)

where the state  $x(t) = [x_1(t), x_2(t), \dots, x_n(t)]^{\mathsf{T}}$ , the matrix

$$A = \begin{bmatrix} 0 & 1 & 0 & \cdots & 0 \\ 0 & 0 & 1 & \cdots & 0 \\ \vdots & \vdots & & \vdots & \\ 0 & -a_{n-1} & -a_{n-2} & \cdots & -a_1 \end{bmatrix}$$

and the vector  $b = [0, 0, \ldots, a_{n-1}]^\mathsf{T}$ , with  $a_i > 0$ ,  $i = 1, 2, 3, \ldots$ , n-1,  $x_0 = [x_{10}, x_{20}, \ldots, x_{n0}]^\mathsf{T}$  is the initial condition, and  $x_{2c}(t)$  is the rate command. Assume that the pilot's reference rate command r(t) is a bounded positive signal with lower bound  $r_0 > 0$  and upper bound  $r_m$ . The control design objective is to develop a command limiting signal  $x_{2c}(t)$  such that the state  $x_1(t)$  converges to a design value  $X_d$  below the limit  $X_m$ .

In this study, the command limiting control law consists of two components, the original reference command r(t) and the protection command  $r_p(t)$ , such that

$$x_{2c}(t) = r(t) + r_p(t)$$
 (2)

In the next section, the command limiting design based on exponential potential functions will be discussed.

## III. Command Limiting Design Using Exponential Potential Functions

In this section, an exponential repulsive potential function is proposed to develop the command limiting control law, followed by stability analysis and some discussion on a tuning parameter.

#### A. Command Limiting Control Law

Let  $h = [1, \zeta_1, \zeta_2, \dots, \zeta_{n-1}]^T$ , where  $\zeta_i \in \mathbb{R}$ ,  $i = 1, 2, \dots, n-1$  are design parameters to be chosen. Consider the following exponential repulsive potential function:

$$U_{\text{rep}}(x(t)) = e^{\eta h^{\mathsf{T}} x(t)} \tag{3}$$

where  $\eta$  is a positive tuning parameter taking values in a neighborhood of 1. The protection control law is then generated by the following gradient descent law:

$$r_p(t) = \beta(t) \frac{\partial U_{\text{rep}}(x)}{\partial x_1} = \beta(t) \eta e^{\eta h^{\mathsf{T}} x(t)} \tag{4}$$

The following total command limiting control signal can be obtained:

$$x_{2c}(t) = r(t) + r_p(t) = r(t) \left(1 - e^{\eta(h^{\mathsf{T}}x(t) - X_d)}\right)$$
 (5)

if  $\beta(t)$  is chosen as

$$\beta(t) = -\frac{r(t)}{ne^{(\eta X_d)}}\tag{6}$$

It will be shown in the stability analysis that if  $\zeta_i$ , i = 1, 2, ..., n-1, satisfy some conditions, the state  $x_1(t)$  will converge to the value  $X_d$  for the given positive reference command r(t).

In the following part, some fundamental properties of the exponential function will be discussed for a better understanding of the control law. In the discussion, the tuning parameter  $\eta$  is set to 1 for simplicity and the conclusion extends to  $\eta$  in a neighborhood of 1. Consider the command limiting control law given in Eq. (5) with  $\eta=1$  for the system in Eq. (1). Properties of the exponential function indicate that when  $h^{\mathsf{T}}x(t)$  is much smaller than  $X_d$ , the exponential term is close to zero and the following holds:

$$1 - e^{(h^{\mathsf{T}}x(t) - X_d)} \approx 1, \qquad h^{\mathsf{T}}x(t) \ll X_d \tag{7}$$

In this case, the total command is approximately equal to r(t) and the state  $x_2(t)$  will track the command signal r(t) with a satisfactory performance from the CAS. The effect of the protection command on the reference command is negligible.

As  $x_1(t)$  increases and approaches  $X_d$  and consequently  $(h^T x(t) - X_d)$  approaches zero, the magnitude of the exponential term increases. The total command can be written as

$$x_{2c}(t) = -K(x(t), t)(h^{\mathsf{T}}x(t) - X_d)$$
 (8)

where

$$K(x(t), t) = r(t) \sum_{n=1}^{\infty} \frac{(h^{\mathsf{T}}x(t) - X_d)^{n-1}}{n!}$$

Since it can be verified that

$$\sum_{n=1}^{\infty} \frac{x^{n-1}}{n!} > 0, \quad \forall \ x \in \mathbb{R}$$
 (9)

this control law is equivalent to a state feedback control law with a time-varying gain whose magnitude increases as the value of  $(h^{\top}x(t) - X_d)$  increases. Hence, when the protected state approaches  $X_d$ , the gain will increase, resulting in a faster convergence of  $x_1(t)$  to  $X_d$ . In the next part, the stability of the closed-loop system will be analyzed.

#### B. Stability Analysis

With the command limiting control law defined in Eq. (5), the following closed-loop system can be obtained:

$$\dot{x}(t) = Ax(t) + br(t) \Big( 1 - e^{\eta(h^{\mathsf{T}}x(t) - X_d)} \Big), \qquad x(0) = x_0 \quad (10)$$

which has an equilibrium at  $x_e = [X_d, 0, \cdots, 0]^T$ . For stability analysis, a change of coordinates is conducted to move the equilibrium to the origin, and the following system is obtained (note that the original notations are retained to represent the new states after the change of coordinates):

$$\dot{x}(t) = Ax(t) + br(t) \Big( 1 - e^{\eta h^{\mathsf{T}} x(t)} \Big), \qquad x(0) = x_0 - x_e$$
 (11)

To facilitate the stability analysis, define a symmetric matrix

$$P_n = [p_{i,j}]_{i,j=1}^n \tag{12}$$

where  $p_{i,j} = p_{j,i}$ ,  $p_{1,n} = 1$ , and  $p_{i+1,n} = \zeta_i$ , for i = 1, 2, 3, ..., n-1, and  $\zeta_i$ 's were introduced previously. Let  $\zeta_0 = 1$ . Further let

$$p_{i,j} = p_{i,n} a_{n-j} + p_{j+1,n} a_{n+1-i} - p_{i-1,j+1}, \quad 1 \le i \le j < n \quad (13)$$

and  $p_{i,j} = 0$  otherwise. For the system in Eq. (11), pick  $\zeta_i$ , i = 1, 2, ..., n-1, such that the following conditions are satisfied:

$$p_{i,i+1} - \zeta_i a_{n-i} < 0, \qquad i = 1, 2, 3, \dots, n-1$$
 (14)

which can be expanded as

$$\begin{cases}
a_{n-2} < \zeta_1 a_{n-1}, \\
\zeta_1 a_{n-3} + \zeta_3 a_{n-1} - p_{1,4} < \zeta_2 a_{n-2}, \\
\vdots \\
\zeta_{n-2} < \zeta_{n-1} a_1
\end{cases} (15)$$

The following theorem about the stability of the system in Eq. (11) holds:

Theorem 1: If there exist  $\zeta_i$ , i = 1, 2, ..., n - 1, satisfying the inequalities in Eq. (15) such that the following command signal stabilizes the system in Eq. (1)

$$x_{2c}(t) = -r_0 h^{\mathsf{T}} x(t) \tag{16}$$

then the system in Eq. (11) is globally uniformly exponentially stable. *Proof:* The proof is in the Appendix.

*Remark:* In general, a full state feedback defined in Eq. (16) exists for an aerial vehicle equipped with an angular rate CAS such that an attitude tracking controller can be developed for the vehicle. To implement the proposed command limiting design successfully, numerical optimization methods can be conducted to find  $\zeta_i$ 's, which satisfy the inequalities in Eq. (15) and yield a controller with good performance.

#### C. Role of the Tuning Parameter

Recall that the potential function was defined by

$$U_{\rm ren}(x(t)) = e^{\eta h^{\mathsf{T}} x(t)} \tag{17}$$

and the total command is generated by

$$x_{2c}(t) = r(t) \left( 1 - e^{\eta(h^{\mathsf{T}}x(t) - X_d)} \right)$$
 (18)

In this control law, the positive  $\eta$  affects where the FEP law starts to make significant modifications to the reference command r(t). It also

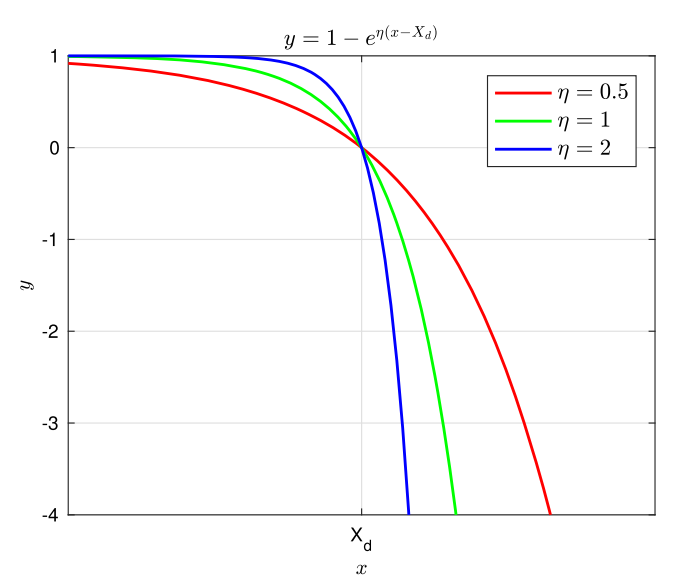


Fig. 1 Plots of  $y = 1 - e^{\eta(x - X_d)}$ .

affects the rate of convergence of  $x_1(t)$ . The idea is illustrated in Fig. 1. The figure shows the plot of the function  $y=1-e^{\eta(x-X_d)}$  with  $\eta=0.5,1$ , and 2. From these plots, one can notice that with a larger  $\eta$ , the protection command will start to generate significant corrections at a larger x value, and the total command will be steeper close to the design value  $X_d$ . With a smaller  $\eta$ , the modification starts farther from the limit and the total control command is smaller. The role of this coefficient will be further shown in simulations.

# IV. Simulation Example: Pitch-Angle Protection for a UAV Model

In this section, the effectiveness of the proposed envelope protection method is verified via simulation study. The protection of pitch angle  $\theta(t)$  for a UAV is considered. The UAV model used in this simulation was developed by the Uninhabited Aerial Vehicle Laboratories at the University of Minnesota [31]. This high-fidelity simulation can model nonlinear bare airframe dynamics, actuator dynamics, and measurement uncertainties. It is an appropriate simulation environment to test the proposed command limiting design. More information on this UAV model can be found in [32]. For this UAV model, a pitch-rate CAS is designed based on a linear model obtained at a trim condition with a speed of 23 m/s at an altitude of 200 m, and then the command limiting design is implemented. The speed controller and bank angle controller associated with the model are used without modifications to maintain the forward speed and zero bank angle during the simulation.

The pitch-rate CAS accepts pitch-rate command  $q_c(t)$  and is developed based on the short-period mode of this model. The pitch-rate CAS control law is given by

$$u_{\text{cas}}(t) = K_a q(t) + K_I x_I(t)$$
 (19)

where q(t) is the pitch rate of the UAV, and  $x_I(t) = \int_0^t q_c(\tau) - q(\tau) d\tau$  is the integrator state. With this CAS, the equations of motion of the system with states  $\theta(t)$ , q(t), w(t), and  $x_I(t)$  are written below:

$$\begin{bmatrix} \dot{\theta} \\ \dot{q} \\ \dot{w} \\ \dot{x}_I \end{bmatrix} = \begin{bmatrix} 0 & 1 & 0 & 0 \\ 0 & -15.51 & -1.673 & 61.86 \\ -0.8066 & 21.90 & -6.359 & 8.176 \\ 0 & -1 & 0 & 0 \end{bmatrix} \begin{bmatrix} \theta \\ q \\ w \\ x_I \end{bmatrix} + \begin{bmatrix} 0 \\ 0 \\ 0 \\ 1 \end{bmatrix} q_c$$
(20)

where w(t) is the speed along z axis of the body frame. Let the state vector be  $x(t) = [\theta(t), q(t), w(t), x_I(t)]^{\mathsf{T}}$ . Assume that the positive limit for the pitch angle is  $\theta_d = 20\,$  deg. With the command limiting control law and a positive pitch rate reference command, the system will converge to an equilibrium. At the equilibrium point, we have  $\theta_e = \theta_d$  and  $q_e = 0$ . Then we can solve for  $w_e$  and  $x_{Ie}$  for this point. Let  $x_e$  denote this equilibrium point. Consider the following command limiting control law:

$$q_c(t) = q_r(t) \left( 1 - e^{\eta(h^{\mathsf{T}}x(t) - X_d)} \right) \tag{21}$$

where  $X_d = h^{\mathsf{T}} x_e$  and  $q_r(t)$  is the reference command. The equilibrium point  $x_e$  can be shifted to the origin by a change of coordinates. For this shifted system, there exists a similarity transformation z(t) = Tx(t), which transforms it into

$$\begin{bmatrix} \dot{z}_1 \\ \dot{z}_2 \\ \dot{z}_3 \\ \dot{z}_4 \end{bmatrix} = \begin{bmatrix} 0 & 1 & 0 & 0 \\ 0 & 0 & 1 & 0 \\ 0 & 0 & 0 & 1 \\ 0 & -a_{z3} & -a_{z2} & -a_{z1} \end{bmatrix} \begin{bmatrix} z_1 \\ z_2 \\ z_3 \\ z_4 \end{bmatrix} + \begin{bmatrix} 0 \\ 0 \\ 0 \\ 1 \end{bmatrix} q_c \quad (22)$$

For stability analysis, note that the command limiting control law becomes

$$q_c(t) = q_r(t) \left( 1 - e^{\eta h^T T^{-1} z(t)} \right)$$
 (23)

 $\begin{cases}
 a_{z3}\zeta_1 > a_{z2}, \\
 a_{z2}\zeta_2 > a_{z1}\zeta_1 + a_{z3}\zeta_3 - 1, \\
 a_{z1}\zeta_3 > \zeta_2
\end{cases} (24)$ 

Let  $h_z^{\mathsf{T}} = h^{\mathsf{T}} T^{-1} = d \cdot [1, \zeta_1, \zeta_2, \zeta_3]$ , where d is equal to the first element of  $h_z$  and is used to normalize the result. The conditions for  $\zeta_1, \zeta_2$ , and  $\zeta_3$  from Eq. (15) are

Choose appropriate values for h such that these conditions on  $\zeta_1$ ,  $\zeta_2$ , and  $\zeta_3$  are satisfied. Then the following Lyapunov function

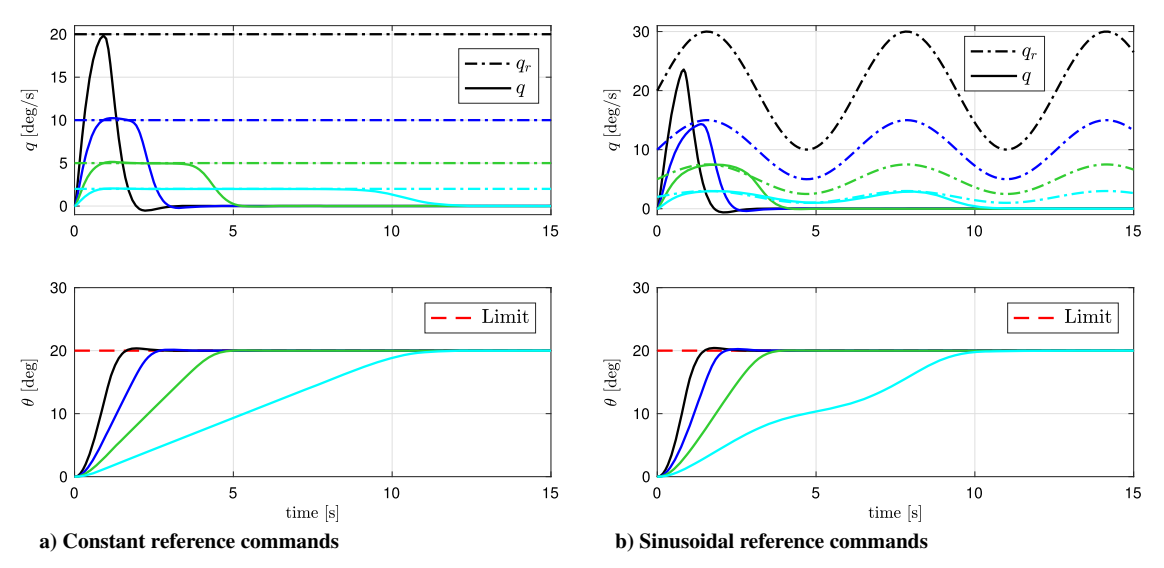


Fig. 2 Pitch-rate command limiting for pitch-angle protection: linearized model.

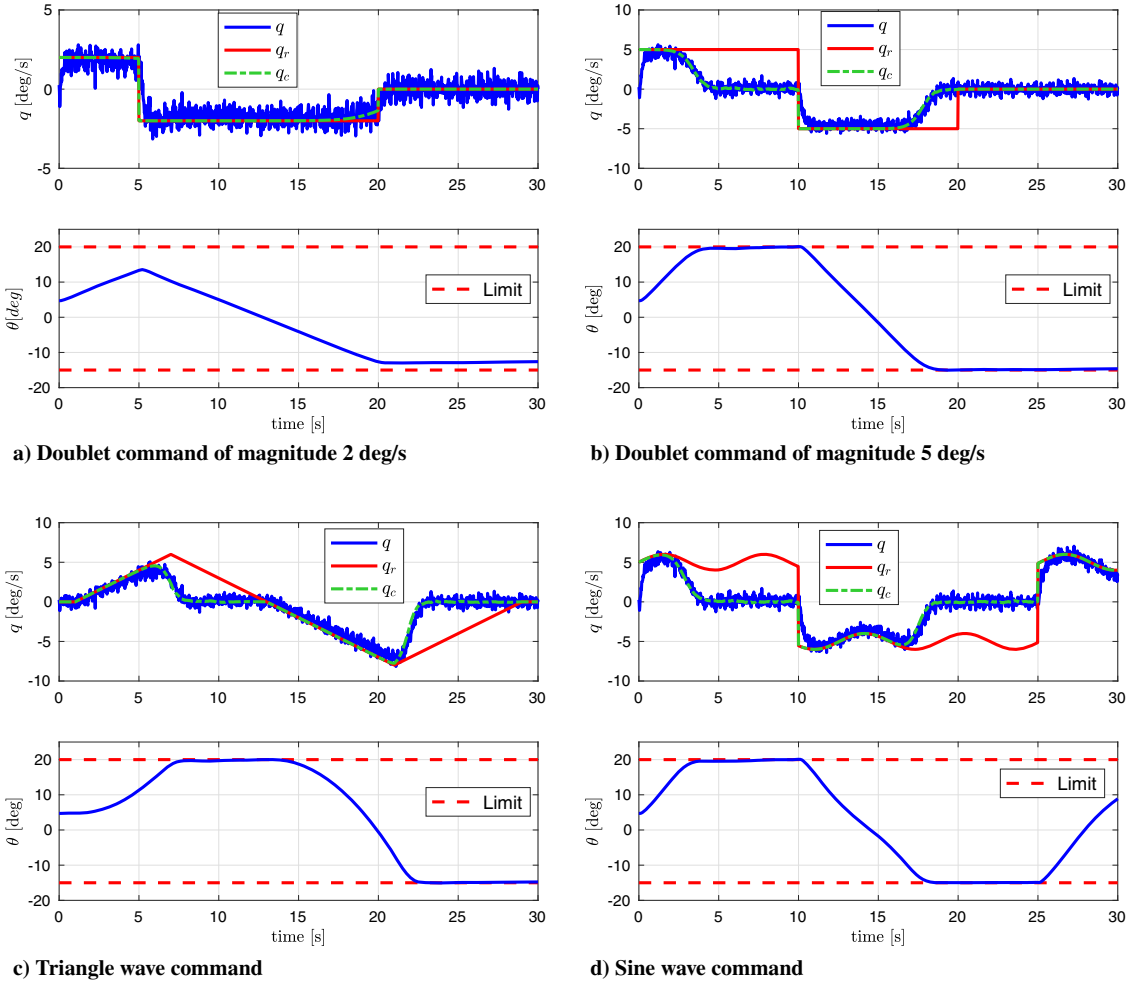


Fig. 3 Pitch-rate command limiting for pitch-angle protection: responses to various reference commands.

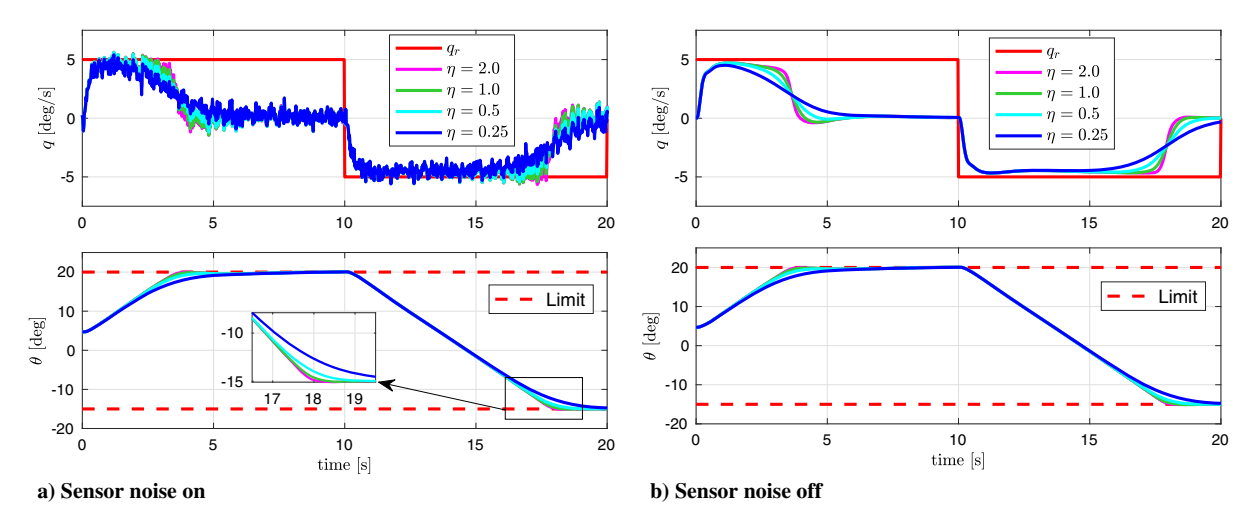


Fig. 4 Pitch-rate command limiting for pitch-angle protection: responses with different  $\eta$ 's.

$$V(z) = \frac{1}{2} z^{\mathsf{T}} P_4 z \tag{25}$$

where

$$P_{4} = \begin{bmatrix} a_{z3} & a_{z2} & a_{z1} & 1\\ a_{z2} & \zeta_{1}a_{z2} + \zeta_{2}a_{z3} - a_{z1} & \zeta_{1}a_{z1} + \zeta_{3}a_{z3} - 1 & \zeta_{1}\\ a_{z1} & \zeta_{1}a_{z1} + \zeta_{3}a_{z3} - 1 & \zeta_{2}a_{z1} + \zeta_{3}a_{z2} - \zeta_{1} & \zeta_{2}\\ 1 & \zeta_{1} & \zeta_{2} & \zeta_{3} \end{bmatrix} > 0$$

$$(26)$$

can be used to show that the closed-loop system is exponentially stable.

In the following simulation example with the linearized system,  $h = [1, 0, 0, 1.01]^T$  and  $\eta = 1$  are used. Simulation results are shown in Fig. 2. Simulation results indicate that the proposed method can provide effective command limiting performance for both constant and time-varying reference commands on this linear system.

Next, nonlinear simulation results are presented. The positive limit of the pitch angle is again  $\theta_d=20\,$  deg and the negative limit is set to  $\theta_d^-=-15\,$  deg. Sensor noise is added to the simulation for high fidelity. Note that the negative command limiting design is developed based on the same idea and then integrated with the positive command limiting control law. The total command is defined as

$$q_{c}(t) = \begin{cases} q_{r}(t) \left( 1 - e^{\eta(h^{\mathsf{T}}x(t) - X_{d})} \right), & \text{if } q_{r}(t) \ge 0, \\ q_{r}(t) \left( 1 - e^{-\eta(h^{\mathsf{T}}x(t) - X_{d}^{-})} \right), & \text{if } q_{r}(t) < 0 \end{cases}$$
(27)

where  $X_d^-$  can be obtained similarly as  $X_d$  for the negative limit. For the nonlinear model,  $\eta=0.5$  and the same h is used. One can notice that if the reference command  $q_r(t)$  is nonnegative, the protection for  $\theta_d$  is effective; otherwise, the protection for  $\theta_d^-$  is effective. When the state is far away from either limit, the correction to the pilot command is negligible due to the property of the exponential function.

Figure 3 presents the time responses of the UAV model to various reference commands. Figure 3a indicates that when the magnitude of the reference command is small and the protected state is far away from the limit, the total command  $q_c(t)$  is almost identical to the reference command  $q_r(t)$ , and the effect of the command limiting component is negligible. Figure 3b shows the response to a reference command with larger magnitude. As the protected state  $\theta(t)$  approaches the limit, the command limiting component takes effect and modifies the reference command  $q_r(t)$  such that the protected state  $\theta(t)$  converges to the design values  $\theta_d$  or  $\theta_d^-$ , and hence envelope protection is achieved. Figures 3c and 3d depict the responses to a triangle wave and a sine wave reference command, respectively. The

command limiting control law works as expected and provides effective envelope protection in both cases.

To further show the role that the tuning parameter  $\eta$  plays in the performance of the command limiting control law, Fig. 4 presents the time responses of the UAV model augmented with the command limiting control law using different  $\eta$ 's. As discussed earlier, the value of  $\eta$  influences the point where the command limiting control law takes significant effect, as well as the rate of convergence of the protected state (here  $\theta$ ). These two figures further verify these conclusions. With a smaller  $\eta$ , the correction to the reference command starts at a point farther from the envelope limit than with a larger  $\eta$ , the modification to the reference command changes slower, and the rate of convergence of the protected state is smaller. This also implies an earlier interference with pilot operations. With a larger  $\eta$ , the protection is initiated closer to the limit and a faster correction to the reference command is made. The plots also suggest that when  $\eta$ becomes larger than 1, the difference between responses becomes smaller: for example, the difference between  $\eta = 1$  and  $\eta = 2$  is very small. Hence,  $\eta$  can be tuned in a proper neighborhood of 1.

#### V. Conclusions

In this study, a command limiting control law for FEP based on exponential potential functions was proposed. In the design, the reference command was treated as an attractive potential function, and repulsive potential functions were designed such that as the protected state approached the envelope limit, the value of the repulsive potential function increased, generating a protection signal to reduce the reference command and provide envelope protection. The protection command can be merged with the reference command due to the property of exponential functions. The contribution of the protection command remains negligible when the protected state is far from the limit, but increases as the limit approaches. The tuning parameter can adjust the position where the command limiting control law starts to make significant correction to the reference command. Lyapunov stability theory was employed to analyze the closed-loop system with the proposed command limiting design, and simulation examples in a nonlinear UAV simulation environment were presented to verify the effectiveness of the design.

#### **Appendix: Proof of Theorem 1**

*Proof of Theorem 1:* Consider the symmetric matrix  $P_n$  defined in Eqs. (12) and (13). First we show that the symmetric matrix  $P_n$  is positive definite by studying the closed-loop system consisting of the system in Eq. (1) and the command signal defined in Eq. (16). The closed-loop system is written below:

$$\dot{x}(t) = Ax(t) - br_0 h^{\mathsf{T}} x(t), \qquad x(0) = x_0$$
 (A1)

which can be further written as

$$\dot{x}(t) = A_0 x(t), \qquad x(0) = x_0$$
 (A2)

where  $A_0 = A - br_0 h^{\mathsf{T}}$ .

Consider the following Lyapunov function candidate:

$$V(x) = \frac{1}{2} x^{\mathsf{T}} P_n x \tag{A3}$$

The time derivative of the Lyapunov function candidate is then

$$\dot{V}(x) = \frac{1}{2}\dot{x}^{\mathsf{T}}P_{n}x + \frac{1}{2}x^{\mathsf{T}}P_{n}\dot{x} = \frac{1}{2}x^{\mathsf{T}}(A_{0}^{\mathsf{T}}P_{n} + P_{n}A_{0})x$$

$$= \sum_{i=2}^{n} x_{i}^{2}(p_{i-1,i} - \zeta_{i-1}a_{n-i+1})$$

$$+ \sum_{\substack{i,j=1\\i < j}}^{n} x_{i}x_{j}(p_{i-1,j} + p_{i,j-1} - p_{i,n}a_{n-j+1} - p_{j,n}a_{n-i+1})$$

$$- a_{n-1}r_{0}(x_{1} + \zeta_{1}x_{2} + \dots + \zeta_{n-1}x_{n})^{2} \tag{A4}$$

Equation (13) guarantees that the coefficients of the cross terms  $x_i x_j$ , i < j, are zero. Hence

$$\dot{V}(x) = \sum_{i=2}^{n} x_i^2 (p_{i-1,i} - \zeta_{i-1} a_{n-i+1})$$
$$- a_{n-1} r_0 (x_1 + \zeta_1 x_2 + \dots + \zeta_{n-1} x_n)^2$$
(A5)

The conditions in Eq. (14) on  $\zeta_i$ 's assure that the coefficients of the square terms  $x_i^2$ ,  $i=2,3,\ldots,n$ , are negative, and this implies that the time derivative of the Lyapunov function candidate is negative definite. In fact, the time derivative of the Lyapunov function can be further written as

$$\dot{V}(x) = -x^{\mathsf{T}} Q_n^{r_0} x \tag{A6}$$

where  $Q_n^{r_0}$  is positive definite with its elements defined by

$$Q_{nii}^{r_0} = \begin{cases} a_{n-1}r_0, & i = 1, \\ \zeta_{i-1}a_{n-i+1} - p_{i-1,i} + a_{n-1}\zeta_{i-1}^2r_0, & i > 1, \end{cases}$$

$$Q_{nij}^{r_0} = \begin{cases} a_{n-1}\zeta_{j-1}r_0, & i = 1, j > i, \\ a_{n-1}\zeta_{i-1}\zeta_{j-1}r_0, & i > 1, j > i \end{cases}$$
(A7)

Hence the following equation holds:

$$A_0^{\mathsf{T}} P_n + P_n A_0 = -2Q_n^{r_0} \tag{A8}$$

Since the closed-loop linear system in Eq. (A1) is assumed to be exponentially stable and  $Q_n^{r_0}$  is positive definite, the symmetric matrix  $P_n$  is positive definite [33].

Next, we show that the nonlinear system in Eq.  $(\underline{11})$  is exponentially stable. Consider the same Lyapunov function candidate defined in Eq.  $(\underline{A3})$ . The time derivative of the Lyapunov function candidate for the system in Eq.  $(\underline{11})$  is

$$\dot{V}(x) = \sum_{i=2}^{n} x_i^2 (p_{i-1,i} - \zeta_{i-1} a_{n-i+1}) 
+ \sum_{\substack{i,j=1\\i < j}}^{n} x_i x_j (p_{i-1,j} + p_{i,j-1} - p_{i,n} a_{n-j+1} - p_{j,n} a_{n-i+1}) 
+ a_{n-1} r(t) (h^{\mathsf{T}} x) (1 - e^{\eta h^{\mathsf{T}} x})$$
(A9)

Similarly, Eq. (13) guarantees that the coefficients of the cross terms  $x_i x_i$ , i < j, are zero. Hence

$$\dot{V}(x) = \sum_{i=2}^{n} x_i^2 (p_{i-1,i} - \zeta_{i-1} a_{n-i+1}) + \frac{a_{n-1} r(t)}{\eta} (\eta h^{\mathsf{T}} x) (1 - e^{\eta h^{\mathsf{T}} x})$$
(A10)

The conditions in Eq. (14) on  $\zeta_i$ 's again assure that the coefficients of the square terms  $x_i^2$ , i = 2, 3, ..., n, are negative.

Next we verify that given  $r(t) > r_0 > 0$ ,  $\forall t \ge 0$ , the second term in the above time derivative of the Lyapunov function candidate is negative semidefinite, which is equivalent to

$$(\eta h^{\mathsf{T}} x)(1 - e^{\eta h^{\mathsf{T}} x}) \le 0, \quad \forall \ x \in \mathbb{R}^n$$
 (A11)

Consider the following function of *y*:

$$f(y) := (1 - e^y)y, \qquad y \in \mathbb{R} \tag{A12}$$

The first and second derivatives of this function with respect to y are then

$$f'(y) = 1 - e^{y}(y+1), \quad f''(y) = -e^{y}(y+2)$$
 (A13)

which implies that  $f'(y) = 0 \Leftrightarrow y = 0$  and f''(0) = -2. This indicates that f(y) attains its global maximum at y = 0 and f(0) = 0. Hence we conclude that

$$f(y) = (1 - e^y)y \le 0, \quad \forall \ y \in \mathbb{R}$$
 (A14)

Based on this result, the following inequality holds:

$$(\eta h^{\mathsf{T}} x)(1 - e^{\eta h^{\mathsf{T}} x}) \le 0, \quad \forall \ x \in \mathbb{R}^n$$
 (A15)

Then, if the conditions in Eq.  $(\underline{14})$  hold, the following result can be obtained:

$$\dot{V}(x) \le \sum_{i=2}^{n} x_i^2 (p_{i-1,i} - p_{i,n} a_{n-i+1}) \le 0$$
 (A16)

Hence, the system in Eq. (11) is uniformly stable [34]. This also suggests that for any  $\epsilon > 0$  there exists  $\delta = \delta(\epsilon)$  such that

$$||x(0)|| < \delta \Rightarrow ||x(t)|| < \epsilon, \quad \forall \ t \ge 0$$
 (A17)

Consider the function f(y) defined in Eq. (A12) again. In the following, we show that within a neighborhood of the origin, the function f(y) is bounded from above by some negative quadratic function. That is, for any  $\varepsilon_y > 0$ , there exists  $c = c(\varepsilon_y) > 0$  such that

$$|y| < \epsilon_v \Rightarrow f(y) \le -cy^2$$
 (A18)

Figure  $\underline{A1}$  illustrates the intersections of f(y) and  $-cy^2$  for three different values of c, which indicates that such c exists.

Consider the following function g(y):

$$g(y) := f(y) + cy^{2} = (1 - e^{y})y + cy^{2} = y(1 - e^{y} + cy),$$
  

$$y \in \mathbb{R}$$
(A19)

In the following study, let  $c \in (0, 1)$ . For a given  $\epsilon_y$ , one needs to find a c such that  $g(y) \le 0$ . Again, taking the first and second derivative of g(y) yields

$$g'(y) = f'(y) + 2cy = 1 - e^{y}(y+1) + 2cy,$$
  

$$g''(y) = f''(y) + 2c = -e^{y}(y+2) + 2c$$
(A20)

One of the solutions to g'(y) = 0 is y = 0. Since g''(y) < 0,  $\forall y \ge 0$  and g'(0) = 0, then g'(y) < 0,  $\forall y > 0$ , and hence  $f(y) \le -cy^2$ ,  $\forall y \ge 0$ . One solution to g(y) = 0 is y = 0, and the other solution satisfies

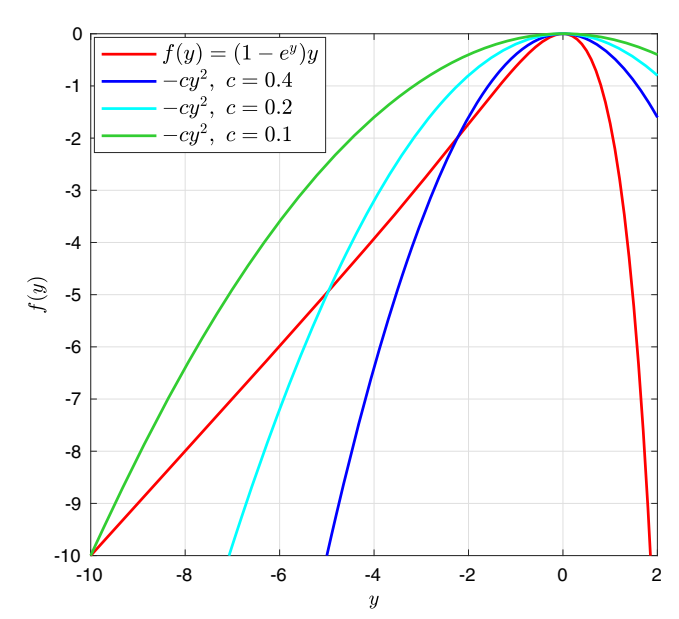


Fig. A1 Plots of f(y) and  $-cy^2$ .

$$1 - e^y + cy = 0 \tag{A21}$$

Hence, given  $y = -\epsilon_y < 0$ , by the mean value theorem there exists  $c_{\epsilon} = e^{y_0}$  with  $\epsilon_y < y_0 < 0$  such that the following equation holds:

$$1 - e^{-\epsilon_y} + c_{\epsilon}\epsilon_y = 0 \tag{A22}$$

since Eq. (A21) can be written as

$$c_{\epsilon} \cdot (0 - \epsilon_{y}) = e^{0} - e^{\epsilon_{y}} \tag{A23}$$

Then for any  $y \in [-\epsilon_y, 0]$ , the following inequality holds:

$$1 - e^y + c_e y \ge 0 \tag{A24}$$

Hence, for any  $y \in [-\epsilon_v, 0]$ , the following is true:

$$g(y) = y(1 - e^y + c_e y) \le 0$$
 (A25)

Further, since  $g(y) \le 0$ ,  $\forall y > 0$ , then for  $y \in [-\epsilon_y, \epsilon_y]$  there exists a c such that

$$f(y) \le -cy^2 \tag{A26}$$

The larger the  $\epsilon_v$ , the smaller the  $c(\epsilon_v)$ .

From previous steps of the stability analysis, it has been proved that the state vector satisfies

$$||x(t)|| < \epsilon, \quad \forall \ t \ge 0$$
 (A27)

and consequently the following inequality holds for some positive value  $\epsilon_1$ :

$$|\eta h^{\mathsf{T}} x(t)| < \epsilon_1, \quad \forall \ t \ge 0$$
 (A28)

Hence, there exists  $c = c(\epsilon_1)$  such that

$$(\eta h^{\top} x)(1 - e^{\eta h^{\top} x}) \le -c \cdot (\eta h^{\top} x)^2, \quad \forall \ x \in \mathbb{R}^n \text{ and } |\eta h^{\top} x| < \epsilon_1$$
(A29)

It follows that the time derivative of the Lyapunov function satisfies

$$\dot{V}(x) \leq \sum_{i=2}^{n} x_i^2 (p_{i-1,i} - \zeta_{i-1} a_{n-i+1}) - a_{n-1} \eta c r(t) (h^{\top} x)^2 \quad (A30)$$

Since  $r(t) > r_0 > 0$ , the time derivative of the Lyapunov function further satisfies

$$\dot{V}(x) < \sum_{i=2}^{n} x_i^2 (p_{i-1,i} - \zeta_{i-1} a_{n-i+1}) - a_{n-1} \eta c r_0 (h^{\mathsf{T}} x)^2 = -x^{\mathsf{T}} Q_n^{\eta} x$$
(A31)

where the positive definite matrix  $Q_n^{\eta}$  is defined by

$$Q_{nii}^{\eta} = \begin{cases} \eta a_{n-1} c r_0, & i = 1, \\ \zeta_{i-1} a_{n-i+1} - p_{i-1,i} + \eta a_{n-1} \zeta_{i-1}^2 c r_0, & i > 1, \end{cases}$$

$$Q_{nij}^{\eta} = \begin{cases} \eta a_{n-1} \zeta_{j-1} c r_0, & i = 1, j > i, \\ \eta a_{n-1} \zeta_{i-1} \zeta_{j-1} c r_0, & i > 1, j > i \end{cases}$$
(A32)

This leads to

$$\dot{V}(x) \le -\lambda_{\min}(Q_n^{\eta}) \|x\|^2 \tag{A33}$$

Since  $P_n$  is positive definite, the following is true:

$$\lambda_{\min}(P_n) \|x\|^2 \le V(x) \le \lambda_{\max}(P_n) \|x\|^2$$
 (A34)

Hence the system is globally uniformly exponentially stable  $[\underline{34}]$ . This completes the proof.

#### Acknowledgments

This research was partially supported by the China Scholarship Council (2011602110), the Zhejiang University-University of Illinois at Urbana-Champaign (ZJU-UIUC) Institute Research Program, the National Aeronautics and Space Administration, the Air Force Office of Scientific Research, and the National Science Foundation (Award No. 1830639 and 1932529).

#### References

- Belcastro, C. M., and Foster, J. V., "Aircraft Loss-of-Control Accident Analysis," AIAA Guidance, Navigation, and Control Conference, AIAA Paper 2010-8004, 2010. https://doi.org/10.2514/6.2010-8004
- [2] Crider, D. A., "Progress in Loss of Control Mitigation," AIAA Modeling and Simulation Technologies Conference, AIAA Paper 2014-1001, 2014. https://doi.org/10.2514/6.2014-1001
- [3] Rogers, C. R., "Pilot Authority and Aircraft Protections," Tech. Rept., Air Line Pilots Assoc., Airworthiness Performance Evaluation and Certification Com., 1999.
- [4] Lombaerts, T., Looye, G., Ellerbroek, J., and Martin, M. R., "Design and Piloted Simulator Evaluation of Adaptive Safe Flight Envelope Protection Algorithm," AIAA Guidance, Navigation, and Control Conference, AIAA Paper 2016-0093, 2016. https://doi.org/10.2514/6.2016-0093
- [5] Falkena, W., Borst, C., Chu, Q., and Mulder, J., "Investigation of Practical Flight Envelope Protection Systems for Small Aircraft," *Journal of Guidance, Control, and Dynamics*, Vol. 34, No. 4, 2011, pp. 976–988. https://doi.org/10.2514/1.53000
- [6] Wilson, J., and Peters, M., "General Aviation Accident Prevention— Basic Envelope Protection, Phase III: Flight Test Results and Recommendations for Future Envelope Protection Systems," Federal Aviation Administration TR DOT/FAA/TC-13/43, Washington, D.C., 2014.
- [7] Tekles, N., Chongvisal, J., Xargay, E., Choe, R., Talleur, D. A., Hovakimyan, N., and Belcastro, C. M., "Design of a Flight Envelope Protection System for NASA's Transport Class Model," *Journal of Guidance, Control, and Dynamics*, Vol. 40, No. 4, 2017, pp. 863–877. https://doi.org/10.2514/1.G001728
- [8] Horn, J., Calise, A., and Prasad, J., "Flight Envelope Limiting Systems Using Neural Networks," 23rd Atmospheric Flight Mechanics Conference, AIAA Paper 1998-4459, 1998. https://doi.org/10.2514/6.1998-4459
- [9] Unnikrishnan, S., and Prasad, J., "Reactionary Automatic Envelope Protection for Autonomous Unmanned Aerial Vehicles," AIAA Atmospheric Flight Mechanics Conference and Exhibit, AIAA Paper 2004-4819, 2004.

https://doi.org/10.2514/6.2004-4819

[10] Tang, L., Roemer, M., Ge, J., Crassidis, A., Prasad, J., and Belcastro, C., "Methodologies for Adaptive Flight Envelope Estimation and

- Protection," AIAA Guidance, Navigation, and Control Conference, AIAA Paper 2009-6260, 2009. https://doi.org/10.2514/6.2009-6260
- [11] Yavrucuk, I., Prasad, J. V. R., and Unnikrishnan, S., "Envelope Protection for Autonomous Unmanned Aerial Vehicles," Journal of Guidance, Control, and Dynamics, Vol. 32, No. 1, 2009, pp. 248-261. https://doi.org/10.2514/1.35265
- [12] Shin, H.-H., Lee, S.-H., Kim, Y.-D., Kim, E.-T., and Sung, K.-J., "Design of a Flight Envelope Protection System Using a Dynamic Trim Algorithm," International Journal of Aeronautical and Space Sciences, Vol. 12, No. 3, 2011, pp. 241–251. https://doi.org/10.5139/IJASS.2011.12.3.241
- [13] Sharma, V., Voulgaris, P. G., and Frazzoli, E., "Aircraft Autopilot Analysis and Envelope Protection for Operation Under Icing Conditions," Journal of Guidance, Control, and Dynamics, Vol. 27, No. 3, 2004, pp. 454-465. https://doi.org/10.2514/1.1214
- [14] Bateman, A., Ward, D., Barron, R., and Whalley, M., "Piloted Simulation Evaluation of a Neural Network Limit Avoidance System for Rotorcraft," 24th Atmospheric Flight Mechanics Conference, AIAA Paper 1999-4252, 1999. https://doi.org/10.2514/6.1999-4252
- [15] Wilson, J., and Peters, M., "General Aviation Envelope Protection Feasibility Study," Federal Aviation Administration TR DOT/FAA/ AR-11/9, Washington, D.C., 2011.
- [16] Mulgund, S., and Zacharias, G., "A Hybrid Neural Network-Fuzzy Logic Limit Protection System for Rotorcraft," Guidance, Navigation, and Control Conference, AIAA Paper 1996-3800, 1996. https://doi.org/10.2514/6.1996-3800
- [17] Sahani, N., and Horn, J., "Command Limiting for Full-Envelope Guidance and Control of Rotorcraft," AIAA Guidance, Navigation, and Control Conference and Exhibit, AIAA Paper 2005-6348, 2005. https://doi.org/10.2514/6.2005-6348
- [18] Well, K., "Aircraft Control Laws for Envelope Protection," AIAA Guidance, Navigation, and Control Conference and Exhibit, AIAA Paper 2006-6055, 2006. https://doi.org/10.2514/6.2006-6055
- [19] Gadient, R., Lavretsky, E., and Hyde, D., "State Limiter for Model Following Control Systems," AIAA Guidance, Navigation, and Control Conference, AIAA Paper 2011-6483, 2011. https://doi.org/10.2514/6.2011-6483
- [20] Hyde, D., Gadient, R., and Lavretsky, E., "Flight Testing the X-48B Angle-of-Attack and Sideslip Limiting System," AIAA Guidance, Navigation, and Control Conference, AIAA Paper 2011-6471, 2011. https://doi.org/10.2514/6.2011-6471
- [21] Tekles, N., Holzapfel, F., Xargay, E., Choe, R., Hovakimyan, N., and Gregory, I. M., "Flight Envelope Protection for NASA's Transport Class Model," AIAA Guidance, Navigation, and Control Conference, AIAA Paper 2014-0269, 2014. https://doi.org/10.2514/6.2014-0269
- Lombaerts, T., Looye, G., Ellerbroek, J., and Martin, M. R., "Design and Piloted Simulator Evaluation of Adaptive Safe Flight Envelope

- Protection Algorithm," Journal of Guidance, Control, and Dynamics, Vol. 40, No. 8, 2017, pp. 1902-1924. https://doi.org/10.2514/1.G002525
- [23] Thaiss, C., McColl, C. C., Horn, J. F., Keller, E. E., Ray, A., Semidey, R., and Phan, N. D., "Rotorcraft Real Time Damage Alleviation Through Load Limiting Control," 55th AIAA/ASME/ASCE/AHS/ASC Structures, Structural Dynamics, and Materials Conference, AIAA Paper 2014-1528, 2014. https://doi.org/10.2514/6.2014-1528
- [24] Sun, D., Li, X., Jafarnejadsani, H., and Hovakimyan, N., "A Flight Envelope Protection Method Based on Potential Functions," AIAA Guidance, Navigation, and Control Conference, AIAA Paper 2017https://doi.org/10.2514/6.2017-1024
- [25] Choset, H., Lynch, K. M., Hutchinson, S., Kantor, G. A., Burgard, W., Kavraki, L. E., and Thrun, S., Principles of Robot Motion: Theory, Algorithms, and Implementations, MIT Press, Cambridge, MA, 2005, Chap. 4.
- [26] Choi, H. J., Atkins, E., and Yi, G., "Flight Envelope Discovery for Damage Resilience with Application to an F-16," AIAA Infotech@Aerospace 2010, AIAA Paper 2010-3353, 2010. https://doi.org/10.2514/6.2010-3353
- [27] Leonard, N., and Fiorelli, E., "Virtual Leaders, Artificial Potentials and Coordinated Control of Groups," Proceedings of the 40th IEEE Conference on Decision and Control (Cat. No. 01CH37228), Vol. 3, Inst. of Electrical and Electronics Engineers, Piscataway, NJ, 2001, pp. 2968-2973. https://doi.org/10.1109/cdc.2001.980728
- [28] Sun, D., and Hovakimyan, N., "A Bank Angle Protection Method Based on Potential Functions for Nonliner Aircraft Model," 17th AIAA Aviation Technology, Integration, and Operations Conference, AIAA Paper 2017-3765, 2017. https://doi.org/10.2514/6.2017-3765
- [29] Falkena, W., Borst, C., and Mulder, J., "Investigation of Practical Flight Envelope Protection Systems for Small Aircraft," AIAA Guidance, Navigation, and Control Conference, AIAA Paper 2010-7701, 2010. https://doi.org/10.2514/6.2010-7701
- [30] Baelen, D. V., Ellerbroek, J., van Paassen, M., and Mulder, M., "Design of a Haptic Feedback System for Flight Envelope Protection," 2018 AIAA Modeling and Simulation Technologies Conference, AIAA Paper 2018-0117, 2018. https://doi.org/10.2514/6.2018-0117
- [31] Taylor, B., "Aircraft Simulation Baseline 2014 v1," Univ. of Minnesota 2014, <a href="http://hdl.handle.net/11299/163869">http://hdl.handle.net/11299/163869</a> Digital Conservancy, [retrieved 22 June 2018].
- [32] Paw, Y. C., "Synthesis and Validation of Flight Control for UAV," Doctoral Thesis, Univ. of Minnesota, Minneapolis, MN, 2009, http:// hdl.handle.net/11299/58727.
- [33] Hespanha, J. P., Linear Systems Theory, 2nd ed., Princeton Univ. Press, Princeton, NJ, 2018, pp. 91-92. https://doi.org/10.23943/9781400890088
- Khalil, H., Nonlinear Systems, 3rd ed., Prentice Hall, Upper Saddle River, NJ, 2002, Chap. 4.

### This article has been cited by:

1. Donglei Sun, Hamidreza Jafarnejadsani, Naira Hovakimyan. 2021. Command Limiting for Aerial Vehicles With Rate Control Augmentation Systems. *IEEE Transactions on Aerospace and Electronic Systems* 57:3, 1702-1712. [Crossref]